Glacial flow of floating marine ice in "Snowball Earth"

Jason C. Goodman and Raymond T. Pierrehumbert
Department of Geosciences, University of Chicago, Chicago, Illinois, USA

Received 9 May 2002; revised 10 February 2003; accepted 23 July 2003; published 2 October 2003.

[1] Simulations of frigid Neoproterozoic climates have not considered the tendency of thick layers of floating marine ice to deform and spread laterally. We have constructed a simple model of the production and flow of marine ice on a planetary scale, and determined ice thickness and flow in two situations: when the ocean is globally ice-covered ("hard snowball") and when the tropical waters remain open ("soft snowball"). In both cases, ice flow strongly affects the distribution of marine ice. Flowing ice probably carries enough latent heat and freshwater to significantly affect the transition into a Snowball Earth climate. We speculate that flowing marine ice, rather than continental ice sheets, may be the erosive agent that created some Neoproterozoic glacial deposits. *INDEX TERMS:* 9619 Information Related to Geologic Time: Precambrian; 1620 Global Change: Climate dynamics (3309); 5416 Planetology: Solid Surface Planets: Glaciation; 3344 Meteorology and Atmospheric Dynamics: Paleoclimatology; *KEYWORDS:* neoproterozoic, glaciation, Snowball Earth, sea ice, climate models, paleoclimate

Citation: Goodman, J. C., and R. T. Pierrehumbert, Glacial flow of floating marine ice in "Snowball Earth," *J. Geophys. Res.*, *108*(C10), 3308, doi:10.1029/2002JC001471, 2003.

1. Introduction

[2] Abundant glacial deposits found in Neoproterozoic rocks imply at least two prolonged periods of ice cover at sea level in the tropics, between 750–700 Ma and 610–590 Ma [*Sohl and Christie-Blick*, 1999; *Schmidt and Williams*, 1995; *Evans*, 2000]. Widespread occurrence of postglacial "cap carbonate" deposits with distinctive carbon isotope signatures [*Knoll et al.*, 1986; *Hoffman et al.*, 1998] suggest that this was a global phenomenon. The appearance of sedimentary iron formations [*Young*, 1976] may indicate ocean anoxia. These facts have led to increased interest in the "Snowball Earth" hypothesis [*Kirschvink*, 1992], which posits that the entire ocean became ice covered.

[3] The high albedo of sea ice makes a totally frozen planet a consistent solution to the global radiation balance equations; however, debate has continued over whether the Earth ever reached such a state, and if so, how it was achieved. The most prominent hypothesis for deglaciation, formulated by *Kirschvink* [1992], invokes the cessation of chemical weathering and photosynthesis when the ocean is frozen; this leads to a rise of atmospheric CO_2 levels. This mechanism requires global sea ice cover to be effective. Changes in solar luminosity and continental configuration [*Chandler and Sohl*, 2000; *Crowley and Baum*, 1993] have been cited to explain why Snowball Earth conditions have not occurred more recently. On the other hand, destabilization of methane clathrates may provide an alternative explanation for post-glacial isotope excursions [*Kennedy et al.*, 2001b] that does not require global glaciation.

0148-0227/03/2002JC001471$09.00

[4] The correct interpretation of Neoproterozoic glacial sequences and carbon isotope excursions is a subject of intense, prolific debate [*Hoffman et al.*, 1998; *Christie-Blick et al.*, 1999; *Hoffman and Schrag*, 1999; *Kennedy et al.*, 2001a; *Hoffman and Schrag*, 2002; *Kennedy et al.*, 2001b; *Hoffman et al.*, 2002; *Kennedy et al.*, 2002; *Halverson et al.*, 2002; *Lubick*, 2002], and must presently be considered unresolved.

[5] To date, Neoproterozoic general circulation model experiments with specified ocean heat transport [*Hyde et al.*, 2000; *Peltier*, 2001; *Crowley and Hyde*, 2001] and coupled model experiments with dynamic ocean heat transport [*Poulsen et al.*, 2001; *Peltier*, 2002] have produced solutions in which the tropics remain ice free. This is inconsistent with *Kirschvink*'s [1992] snowball hypothesis, which requires essentially complete ice cover in order to allow the buildup of atmospheric CO_2 that leads to termination of a snowball episode [*Schrag and Hoffman*, 2001]. This disagreement may be interpreted in two ways: either global glaciation did not, in fact, occur, or else the GCM simulations are inaccurate. Given the limitations of GCMs and the difficulty in interpreting the geological evidence, neither possibility can be eliminated.

[6] Observations of thick, widespread glacial deposits present another obstacle for the Snowball Earth idea [*Christie-Blick et al.*, 1999]. Global ice cover would drastically weaken the hydrologic cycle, limiting the growth of continental ice sheets. While the lengthy glacial intervals predicted by the Snowball Earth hypothesis permit enough time to grow kilometer-thick ice sheets, flow velocities would be slow, reducing the potential for erosion. In addition, most deposits suggest a prolonged period of glacial retreat, but the Snowball Earth mechanism predicts very rapid

deglaciation. This makes it difficult to explain the observed glacial deposits from a Snowball Earth perspective.

[7] If the planet was everywhere covered with a thick layer of ice, it becomes difficult to explain the apparent survival of photosynthetic organisms, especially the relatively fragile eukaryotes [*Gaidos et al.*, 1999]. For marine photosynthesizers to survive, there must have been at least small areas of thin, transparent ice or open water. However, once again, open water is inconsistent with the interrupted-carbon-cycle mechanism for Snowball Earth.

[8] Despite its relevance to biology and geology, the thickness of the sea ice layer on a totally ice-covered world has received relatively little attention. The standard assumption in the past has been that the thickness of the sea ice is limited only by the ability of heat generated beneath the ice to diffuse through the ice sheet [*Hoffman et al.*, 1998; *Gaidos et al.*, 1999]. If one assumes a geothermal heat source of roughly 0.08 W/m^2, a thermal diffusivity of ice of roughly 2.5 W/(m^2 K), and an atmospheric temperature of -40°C, one computes a ice layer roughly 1200 m thick.

[9] *McKay* [2000] provides a more elaborate static thermodynamic model of sea ice. Solar penetration and latent heat released by freezing at the base may increase the sub-ice energy source, thinning the ice. Under favorable conditions, the ice in McKay's model can be as little as 1 m thick. Thus McKay's thin ice provides a "photosynthetic window" beneath which life can continue, without exposing liquid water to the atmosphere.

[10] However, *Warren et al.* [2002] observed that *McKay* [2000] used a poorly constrained broadband solar absorptivity for ice, which permitted solar energy to be absorbed too deep within the ice, causing excessive internal heating. Using a spectral absorption model, they found that thin ice was impossible unless the ice had an albedo of only 0.3. However, a snowball state is probably impossible with such low ice albedo. Thus, they conclude, thin ice probably cannot occur on a totally frozen ocean.

[11] The present work proceeds from the observation that when ice becomes very thick, one must consider its fluid dynamics as well as its thermodynamics. Thick floating ice layers (for example, the Antarctic ice shelves) deform plastically under their own weight, thinning and flowing out horizontally over the ocean [*Thomas and MacAyeal*, 1982]. In Snowball Earth conditions, ice should flow from the poles, where it is thickest, toward the equator, where it is thinner. The term "sea glacier" has been coined to distinguish this ice layer from contemporary sea ice (which is typically too thin to flow), and from ice shelves (which are usually thought of as seaward extensions of a continental ice sheet).

[12] The flow of a global sea glacier under these conditions may have profound effects on the climate of Snowball Earth. As ice flows equatorward from high latitudes, it should promote global glaciation, for several reasons:

[13] 1. If flow velocity is large enough, flowing ice may be able to penetrate into areas where temperatures are above freezing. Can a sea glacier penetrate a significant distance into warm latitudes before melting?

[14] 2. Even if melting is too rapid to allow ice to penetrate far into warm areas, a great deal of heat must be supplied to achieve melting at the terminus of the sea glacier. This tends to cool the air and water at the terminus, making the area more favorable to freezing. An equivalent viewpoint is that equatorward flow of ice achieves a poleward transport of latent heat of freezing, and thus cools the tropics.

[15] 3. The release of meltwater at the flow terminus strengthens the ocean stratification in this area. This limits the penetration depth of the ocean convective mixed layer, allowing the ocean to cool more rapidly, again promoting ice growth in the region.

[16] 4. If the areal extent of ice is increased by equatorward flow, either directly or indirectly, the albedo of the planet rises, leading to further cooling via the ice-albedo feedback.

[17] Coupled GCM simulations do not, at present, model the viscous flow of thick sea ice layers. If the above effects are significant, incorporating them into GCMs would make it easier to attain global glaciation in simulations.

[18] In addition, a moving sea glacier that became grounded upon a shallow bottom would erode the bottom as it flowed, planing it flat and creating large amounts of glacial till. In section 5, we investigate whether sea ice flow could be responsible for the glacially eroded carbonate platforms described by *Hoffman et al.* [1998] and other authors.

2. Model Description

[19] We have developed a one-dimensional, time-evolving model for the evolution of a thick floating ice sheet that combines the features of the thermodynamic model of *McKay* [2000] with an ice-shelf flow model [*Macayeal and Barcilon*, 1988; *Weertman*, 1957].

[20] We must stress that the goal here is to determine whether plastic flow of sea ice is an important process, not to generate accurate predictions of sea-ice thickness. To achieve this, we make extreme simplifications throughout the model; potential consequences of these simplifications are discussed in section 5.1. Most importantly, we neglect most feedbacks of the ice sheet onto the oceanic and atmospheric circulations. A detailed treatment of these important interactions will be pursued in future GCM work.

[21] We begin with an ice thickness budget equation,

$$\frac{\partial}{\partial t}h + \nabla \cdot (\mathbf{v}h) = m_b + m_t \tag{1}$$

$$\frac{\partial}{\partial t}h + \mathbf{v} \cdot \nabla h = m_b + m_t - h\nabla \cdot \mathbf{v}, \tag{2}$$

where h is ice thickness, $\mathbf{v}$ is ice flow velocity, and m_b and m_t are the rates of ice accumulation at the bottom and top of the ice layer, respectively.

[22] Ice sheets tend to deform under their own weight, compressing vertically and stretching laterally. *Macayeal and Barcilon* [1988] and *Weertman* [1957] use a very simple model for the evolution of thickness in a floating ice shelf. Using a Glen flow law to describe the rheology of ice, they find that

$$\nabla \cdot v = \mu^n h^n. \tag{3}$$

The parameters μ and n describe the viscosity of the ice. Here μ depends on the vertical temperature profile through the ice, and is specified in Appendix A; $n = 3$ for the Glen flow law.

[23] The surface accumulation rate m_t consists of three factors: evaporation, precipitation, and melting: $m_t = P - E - M$. We use the annual mean of these quantities, and do not attempt to resolve the seasonal cycle. We prescribe $P - E$ using forcing functions derived from coupled GCM experiments: These are specified in sections 3 and 4.

[24] The melting rate is specified as a function of annual-mean surface air temperature and amplitude of the seasonal cycle of temperature (assumed to be sinusoidal), using a melting degree-day parameterization described by *van de Wal* [1996]. Integrating the degree-day melting equation over the seasonal cycle to obtain mean annual melting rate, we obtain

$$M = \alpha \begin{cases} (T_a - T_f) & T_a - \Delta T > T_f \\ \frac{\Delta T}{\pi}\left[\gamma(1 - \operatorname{acos}(\gamma)) + \sqrt{1-\gamma^2}\right] & T_a - \Delta T < T_f < T_a + \Delta T, \\ 0 & T_a + \Delta T < T_f \end{cases}$$

Here, T_a is the annual-mean air temperature; T_f is the freezing temperature of water ($T_f = 273$ K; we ignore the dependence of T_f on pressure and salinity throughout this work); ΔT is the difference between summer peak air temperature and the annual mean; $\alpha = 2.4$ m/(yr-K), and

$$\gamma = \frac{T_a - T_f}{\Delta T}.$$

[25] When temperatures never fall below freezing, the melting rate is proportional to the annual-mean air temperature relative to freezing. When temperatures never climb above freezing, the melting rate is zero. In between, melting occurs only during part of the year.

[26] We obtain the basal freezing rate m_b by balancing an energy budget at the bottom of the ice. The approach used here is essentially that used by *McKay* [2000]. We assume that heat supplied below a level z within the ice must be balanced by upward vertical conduction of heat through level z,

$$\kappa \frac{\partial}{\partial z} T = S(z) + F_g + \rho_i l m_b, \tag{4}$$

where κ is the thermal diffusivity of ice (in W/m-K), $S(z)$ is the solar radiation absorbed below depth z, F_g is the geothermal heat flux, ρ_i is the density of ice, and l is the latent heat of freezing. We ignore the effect of sub-ice ocean heat transport: The importance of this effect and its consequences are discussed in section 5.1.

[27] Note that we have neglected lateral transport of heat by flowing ice in the above equation. This is appropriate if the following Peclet number is small:

$$Pe = \frac{\rho_i C_{pi} \mathbf{u} \cdot \nabla T}{\kappa \frac{\partial^2 T}{\partial z^2}} \sim \frac{\rho_i C_{pi} U H^2}{\kappa L},$$

where C_{pi} is the specific heat of ice, and H, U, and L are scales for ice thickness, flow velocity, and lateral variations in ice temperature (10^4 km). Since H and U are not yet known, we have assumed a priori that $Pe \ll 1$, and verified that the thickness and flow predicted by our model is consistent with that assumption. In the experiments described below, $Pe \leq 0.05$.

[28] Following *McKay* [2000], $S(z)$ is specified as

$$S(z) = S_0(1-a)(1-r)e^{-z/z_0},$$

where S_0 is the incoming solar radiation, a is the albedo, r is a fraction of sunlight absorbed by surface impurities, and z_0 is a scale height for solar penetration into ice. *Warren et al.* [2002] demonstrate that McKay's value of $z_0 = 0.8$ m is far too large: The best fit to their spectral model is obtained with $z_0 \approx 0.05$ m (S. G. Warren, personal communication, 2002).

[29] We now integrate equation (4) through the ice layer from surface (where $T = T_s$) to bottom (where $T = T_f$), and solve for m_b. Like *Warren et al.* [2002], we neglect the temperature-dependence of κ.

$$m_b = \frac{-\kappa(T_s - T_f) - S_0 z_0 (1-a)(1-r)\left(1 - e^{-h/z_0}\right) - F_g h}{\rho_i l h}. \tag{5}$$

This equation says that ice freezes at the base when the rate of geothermal heat supply to the base of the ice is insufficient to balance the conduction of heat through the ice layer. The ice surface temperature is tied to the imposed surface air temperature T_a, but cannot rise above freezing: $T_s = \min(T_a, T_f)$.

[30] We consider the evolution of the ice thickness equation on the spherical Earth. We ignore the existence of continents, and assume rotational symmetry about the axis and reflection symmetry across the equator. Thus equations (2) and (3) become

$$\frac{\partial}{\partial t} h + \frac{v}{r_0} \frac{\partial}{\partial \theta} h = m_b + m_t - \mu^n h^{n+1} \tag{6}$$

$$\frac{1}{r_0 \sin\theta} \frac{\partial}{\partial \theta} v \sin\theta = \mu^n h^n, \tag{7}$$

where r_0 is the Earth's radius; θ is the colatitude; and v is the meridional flow speed, positive for flow from pole to equator.

[31] *Macayeal and Barcilon* [1988] and *Weertman* [1957] developed the flow equation (3) assuming that the ice was frictionlessly constrained within a channel, so that horizontal flow was in one direction only. However, note that because of the diverging meridians on the sphere, ice in the present model must have both along-flow (meridional) and transverse (zonal) strain components: Ice must stretch zonally as it moves equatorward. Does this render equation (7) invalid? *Weertman* [1957] also considered the case of isotropic strain of an unconfined ice sheet. The only difference in this case is a slight change in the value of μ: the strain in any direction in his unconfined ice sheet differs from the strain of ice in a channel by only a factor of 9/8. Thus an ice shelf is able to accommodate a transverse strain

as large as the along-flow strain with negligible change in h. Thus, so long as the transverse strain does not exceed the along-flow strain, we may use equation (7). We have verified a posteriori that this is the case in the model runs described below.

[32] Discretization and numerical integration of these model equations is relatively simple. The model domain contains 100 h- and v-points from equator to pole, with h-points alternating between v-points. The pole is an h-point; the equator is a v-point. At each time step, the velocity is computed by integrating equation (7), assuming $v = 0$ at the pole. This velocity is used to advect h, using a first-order differencing scheme for the advection operator. Time-stepping is achieved using a Runge-Kutta scheme with an adaptive time step.

3. Experiment 1: Partial Glaciation

[33] In this first model experiment, we supply external forcing parameters consistent with the incomplete glaciation often seen in GCM simulations of Snowball Earth (the "Soft Snowball" situation). We compare the ice thickness and extent with *McKay*'s [2000] static ice model, and investigate whether the ice transports enough heat and moisture to affect GCM simulations of snowball climate.

3.1. Forcing Fields

[34] The model requires us to specify annual-mean surface air temperature (T_a), amplitude of the seasonal cycle, evaporation, precipitation, and insolation. We have chosen these fields based on output from simulations of snowball climate using the FOAM GCM [*Poulsen et al.*, 2001; *Jacob et al.*, 2001]. The forcing functions chosen for the present experiment are analytical functions that give a close fit to the annual-mean, zonal-mean output of the FOAM model.

[35] *Poulsen et al.* [2001] found that ocean heat transport strongly affected ice extent in FOAM. When the atmospheric component was coupled to a full dynamic ocean GCM, open water remained at the tropics. When a local slab mixed layer was used (with or without "copper-plate" horizontal thermal diffusion), total ice cover was achieved. However, version 1.3.2 of FOAM, used by *Poulsen et al.* [2001], contains an inconsistency in the code for evaporation over sea ice. Simulations performed using a new version of FOAM (v1.4.30) give similar results, except that the run with horizontal diffusion in the mixed layer no longer freezes over entirely: Surface air temperatures remain above freezing in the tropics. This underscores the general result that the mixed-layer model is close to the threshold for global glaciation, so that small changes in fluxes or energy budget can tip the balance, especially given the strong positive ice-albedo feedback. The forcing fields used here are based on a FOAM simulation with all parameters identical to *Poulsen et al.* [2001]'s diffusive mixed-layer experiment, but using FOAM version 1.4.30.

[36] The annual-mean surface air temperature is approximately

$$T_a = -52^\circ\mathrm{C} + (66^\circ\mathrm{C})\sin^4(\theta),$$

where θ is colatitude. Temperatures are above freezing equatorward of 70°. The amplitude of the seasonal cycle depends on colatitude as follows:

$$\Delta T = 20^\circ\mathrm{C}\ \cos\theta. \tag{8}$$

[37] Evaporation and precipitation are a very strong function of the position of the ice margin in the FOAM runs. The entire ice layer is a zone of net precipitation, largest at the ice margin, and declining exponentially toward the poles. As the ice margin migrates toward the equator, so does the precipitation field. We have found that

$$P - E = 0.37\mathrm{m/yr}\ e^{(\theta-\theta_i)/10^\circ}$$

provides a very good approximation to the $P - E$ field over ice in the FOAM simulation. Here, θ_i is the colatitude of the ice margin. Note that we assume all precipitation falls as snow.

[38] Archives of S_0, the sub-cloud downwelling shortwave flux, are unavailable in the GCM output; however, we do have access to the net downward solar flux, S_0 (1-a). We want to ensure that a in this expression is always the albedo of ice, rather than water. Thus we use the net solar flux from the non-diffusive mixed-layer FOAM run, which is everywhere ice covered. This substitute is adequate unless there are drastic changes in cloudiness between the two FOAM runs; in any case, solar forcing is a relatively unimportant driver of our ice sheet model. The annual-average net solar flux is approximately

$$S_0(1-a) = 35\mathrm{W/m^2} + (90\mathrm{W/m^2})\sin^2(\theta),$$

Figure 1 plots the various forcing components used in this experiment.

3.2. Results

[39] The model is initialized from an ice-free state, and run to equilibrium (~5000 years). From Figure 2, we see that the model predicts ice about 200 m thick from the pole to the 0°C isotherm. Ice does not penetrate significantly into the melting zone. Also shown in this figure is the equilibrium ice thickness predicted by an equivalent thermodynamic ice model with no flow, i.e., by *McKay*'s [2000] model. In the no-flow model, local thickness equilibrium is achieved by requiring that $m_t = -m_b$, and solving equation (5) for h. If flow toward melting zones is not permitted, ice builds up to much greater thickness; in regions of heavy precipitation, it even becomes unbounded. Glacial flow is very effective at limiting ice thickness.

[40] Figure 3 portrays the flow velocities and latent heat transport of the floating ice sheet. Flow velocities peak at 2 km/year near the ice edge, and the peak poleward latent heat transport is about 0.1 PW. This is not a large value compared to present-day atmospheric and oceanic heat transports (~5 and ~1.5 PW, respectively [*Trenberth and Caron*, 2001]). However, unlike the atmosphere and ocean, the ice extracts all of its heat from a very narrow zone right at the ice margin. There, melting ice can cool the atmosphere and ocean by up to 15 W/m^2. Cooling the ice margin

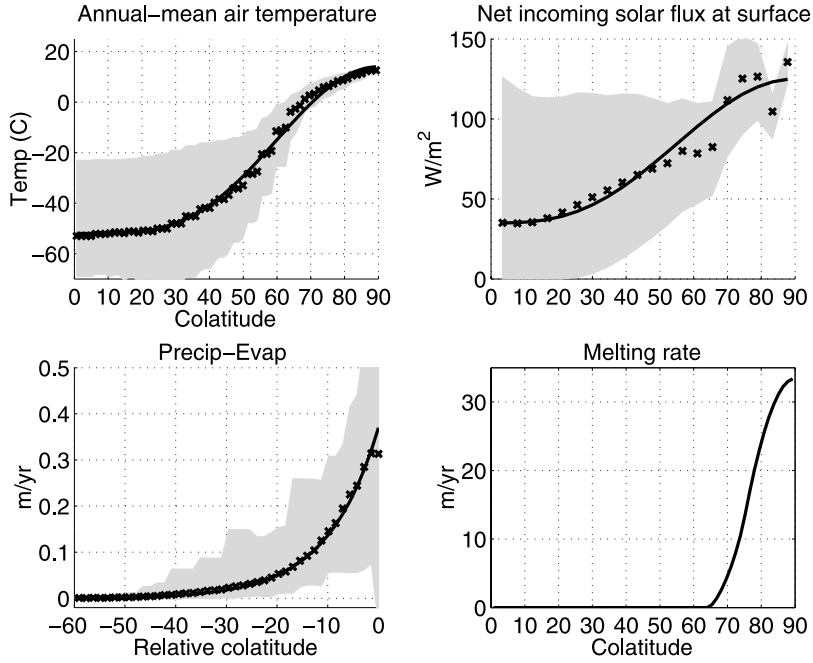

Figure 1. Forcing fields for the partially glaciated experiment. Crosses show zonal and annual-mean output from the Partially glaciated FOAM model run. Solid curves show values used in the present study. Shaded bands show annual variability of FOAM output data, except as noted. (top left) Surface air temperature (T_a), in °C. (top right) Net surface insolation ($S_0(1 - a)$), W/m^2. (bottom left) Precipitation minus evaporation, m/yr. (This field shifts as the ice margin moves: the x axis describes distance in degrees latitude from the ice margin. Shaded band shows range of variability over the FOAM model's 38-year-long transition to equilibrium.) (bottom right) melting rate, m/yr.

promotes further ice growth; in section 5.3, we argue that this cooling is probably a significant factor in the snowball climate.

[41] Figure 4 shows the relative importance of the various terms in the thickness budget equation (6). In high and middle latitudes (0–45° colatitude), the dominant balance is between freezing at the base and thinning via strain. Closer to the melting line (45–63°), basal freezing becomes weaker, but accumulation of snow at the surface more than makes up the difference. Even though the ice is slightly thinner here, its strain is larger because warm ice is more fluid. At 63°, peak summer temperatures rise above freez-

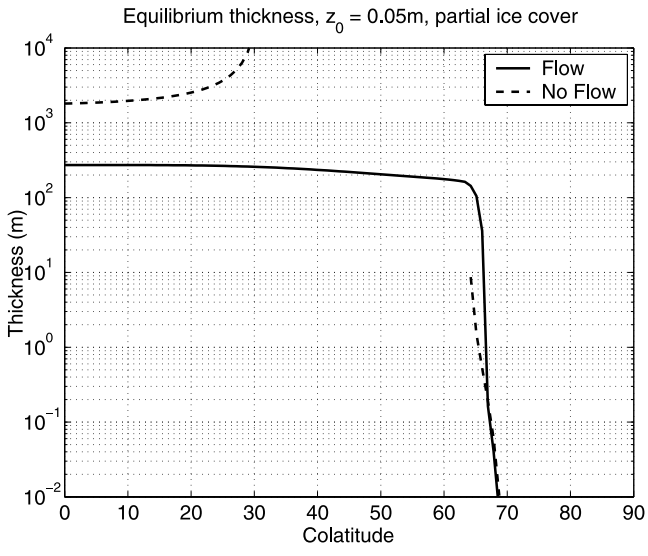

Figure 2. Comparison of equilibrium ice thickness (m) between *McKay*'s [2000] static thermodynamic model (dashed line) and the glacial-flow model (solid line), under partially glaciated forcing conditions.

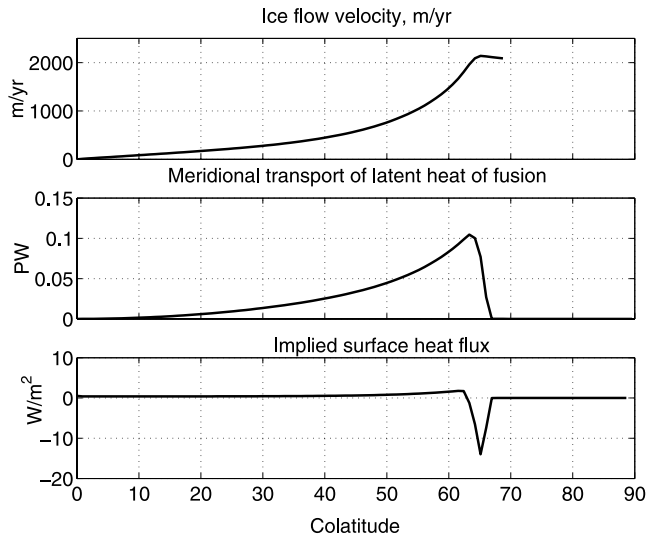

Figure 3. Glacial flow in the partially-glaciated experiment. (top) Flow velocity (m/yr). (middle) Poleward flux of latent heat (PW) by glacial motion ($F_l = 2\pi r_0 l \rho_i \sin(\theta) vh$). (bottom) Surface heat flux (W/m^2) required to balance latent heat flux gain/loss ($H_l = \frac{1}{r_0^2 \sin(\theta)} \frac{\partial}{\partial \theta} F_l \sin(\theta)$).

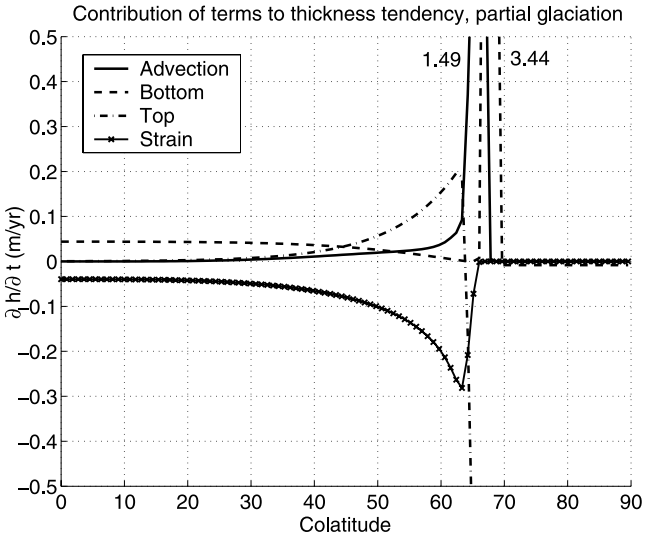

Figure 4. Contribution of terms to the thickness tendency equation (6) for the partially glaciated experiment. "Advection" (solid line) is $-\frac{v}{r_0}\frac{\partial}{\partial\theta}h$; "Bottom" (dashed line) is the bottom freezing/melting rate m_b; "Top" (dash-dotted line) is the surface precipitation/evaporation/melting rate m_t; "Strain" (crosses) is $-a^n h^{n+1}$. Where the curves go off scale, numbers indicate peak values.

ing, and rapid surface melting begins. This melting is balanced only by the advection of ice into the melting zone. The balance between basal freezing and surface melting between 67° and 70° colatitude is an annual-mean view of a seasonally varying sea ice zone: there is a purely local balance between ice melting in the summer, and refreezing in the winter.

[42] We have also computed the freshwater transport via flowing ice (not shown). Equatorward transport of freshwater peaks at about 3.5×10^5 m^3/s (0.35 Sv). This is comparable to the total annual-average present-day atmospheric freshwater flux, which peaks at about 0.7 Sv [*Peixoto and Oort*, 1992]. However, unlike today's atmosphere, all of this freshwater is dumped into the ocean right at the ice margin. From the peak melting flux in Figure 4, the ice delivers as much freshwater to the ice edge as 1.5 m/yr of extra precipitation! In section 5.3, we argue that this huge freshwater flux is expected to promote ice formation by preventing cold, fresh surface water from convectively mixing with warm, salty water beneath the ocean mixed layer.

4. Experiment 2: Global Glaciation

[43] In this section, we consider the thickness and flow of a sea glacier when surface temperatures are everywhere below freezing, and ice cover has become global (the "Hard Snowball" case). Our existing ice flow law (equation (3)) must be modified to consider this case. It predicts positive divergence everywhere; integrating equation (7) with $v = 0$ at the pole gives $v \neq 0$ at the equator, which is inconsistent with the imposed hemispheric symmetry. How do we resolve this? In reality, as the ice sheet in each hemisphere expands to meet its counterpart at the equator, a collision occurs. The derivation of equation (3) assumed that the only force applied at the terminus of the ice shelf was the hydrostatic water pressure. However, now there is an additional back-pressure as ice in each hemisphere pushes on its counterpart across the equator. We demonstrate in Appendix B that the appropriate form of equation (7) is now

$$\frac{1}{r_0 \sin\theta}\frac{\partial}{\partial\theta} v \sin\theta = \mu^n (h - b/h)^n.$$

The back-pressure constant b is a free parameter, which enables the model to satisfy the two boundary conditions $v(\theta = 0) = 0$; $v(\theta = 90°) = 0$. At each time step, our model uses a nonlinear root-finding algorithm to find the value of b necessary to bring the velocity at the equator to zero:

$$v(\theta = 90°) = r_0 \int_0^{\pi/2} \mu^n (h - b/h)^n \sin\theta d\theta = 0.$$

[44] Once b is computed, we can find the strain and velocity everywhere. In areas where ice is thick ($h > \sqrt{b}$), the divergence is positive, and ice spreads and grows thinner. Where ice is thin ($h < \sqrt{b}$), the ice is compressed and thickens. This tends to even out gradients in ice thickness.

4.1. Forcing Fields

[45] For this experiment, we take forcing fields from a FOAM run that does freeze over entirely: the "zero heat flux" run from *Poulsen et al.* [2001], which couples an atmosphere to a local mixed-layer model with zero horizontal diffusion of heat. In this run, the annual-mean surface air temperature is approximately

$$T_a = -54°\mathrm{C} + (33°\mathrm{C}) \sin^4(\theta).$$

Temperatures are everywhere below freezing. The amplitude of the seasonal cycle is taken identical to equation (8).

[46] When liquid water cannot exist, precipitation and evaporation become very small. An approximate fit to the $P - E$ field in the FOAM simulation is

$$P - E = \min(0.01/\phi, -0.015 + 0.03\phi^2)\mathrm{m/yr},$$

where $\phi = (90° - \theta)/25°$. Maximum evaporation is 1.5 cm yr, in the tropics; maximum precipitation is 1.2 cm/yr, near $\theta = 67°$.

[47] Insolation is identical to the partially-glaciated run; surface melting is, of course, zero. Figure 5 plots the various forcing components used in this experiment.

4.2. Results

[48] Ice volume is much larger in this experiment, so a much longer simulation time (~30,000 years) is required to reach equilibrium. Figure 6 shows that the equilibrium ice thickness varies from 1000 m near the pole to 450 m at the equator. In contrast, the static thermodynamic model predicts 2 km of ice at the pole, an unbounded thickness where precipitation is greatest, and 200 m of ice at the equator. Ice flow is very effective at smoothing the ice profile.

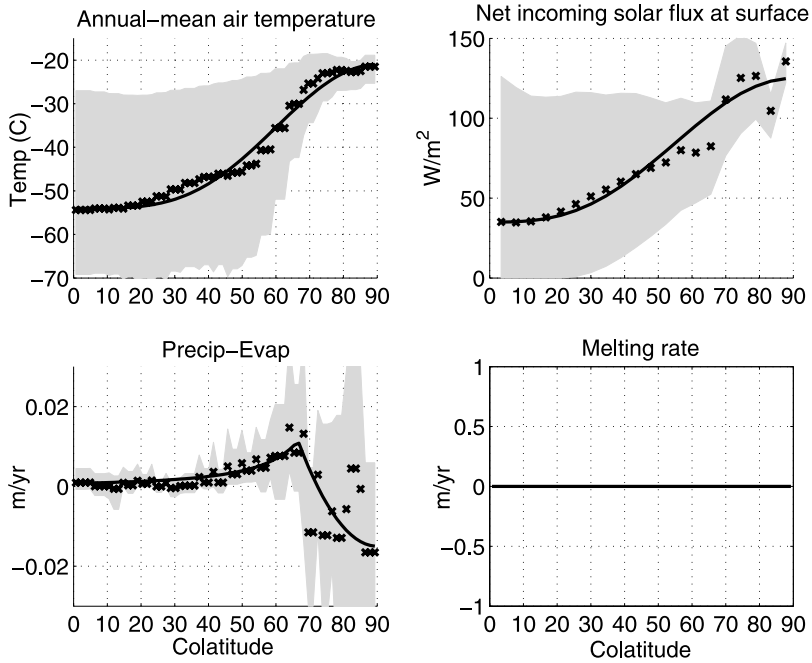

Figure 5. Same as Figure 1, but for the globally glaciated run. Here, $P - E$ is plotted against absolute colatitude, rather than relative to the ice margin.

[49] Figure 7 shows flow velocities and latent heat transport in the ice sheet. The back-pressure at the equator is very effective at retarding ice flow: Maximum velocities in this experiment are only 55 m/yr. Latent heat transport and implied flux are also small: they are probably climatically negligible.

[50] The flow velocity of 55 m/yr can be considered a minimum over a Snowball Earth episode. The FOAM model run describes conditions at the onset of a Snowball Earth period. If *Kirschvink*'s [1992] mechanism is correct, the air temperatures immediately after onset of glaciation were at minimum: Gradual accumulation of atmospheric CO_2 build-up then warmed the planet. As it warmed, the equatorial ice would become thinner, and the back-pressure in equation (4) would drop. This, plus the increased fluidity of warm ice, would cause flow velocities to gradually rise, until the end of the Snowball episode, when flow would be similar to that found in section 4. Supplementary experiments (not shown) demonstrate this effect to be modest. Increasing equatorial air temperature from $-22°C$ to $-5°C$ reduces equatorial ice thickness by 25%; maximum flow velocity increases by 50%.

[51] The balance of terms in the thickness tendency equation is also different (Figure 8). As before, high and middle latitudes are zones of basal freezing and surface accumulation, balanced by thinning of the ice sheet through lateral extension. But in the tropics, ice is thickened by lateral compression; this is balanced by evaporation and basal melting. Advection of thickness gradient is of only minor importance.

5. Discussion

5.1. Model Limitations and Simplifications

[52] The model described here is an extremely simple one, which neglects important interactions between the floating ice and the ocean and atmosphere in order to succinctly describe the dynamics of the ice alone.

5.1.1. Ocean Heat Transport

[53] Perhaps the most significant is the neglect of ocean heat transport beneath the ice. If warm water from the tropics is carried beneath the ice layer and then gives up its heat to the ice, it can produce heat fluxes far in excess of the geothermal input, leading to much thinner ice layers.

[54] This effect is probably not important in the case of a totally ice-covered ocean. In that case, surface waters are at freezing everywhere along the ice/water interface. Since there are no heat sources internal to the fluid, the ocean must be isothermal at the freezing point everywhere, except where

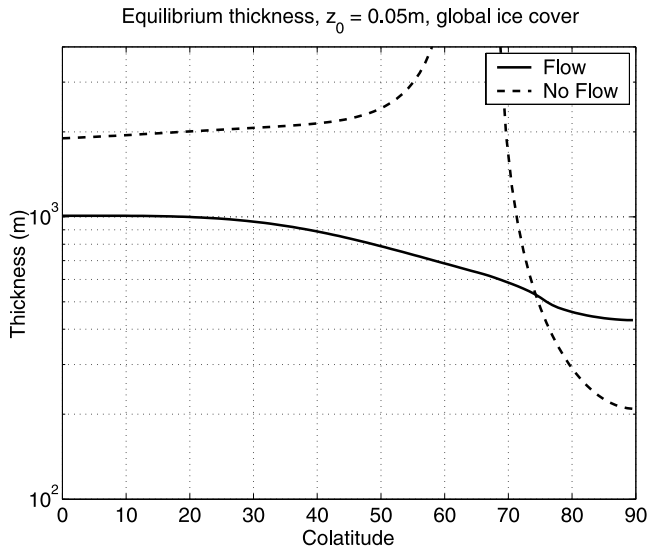

Figure 6. Same as Figure 2, but for the global ice-cover experiment.

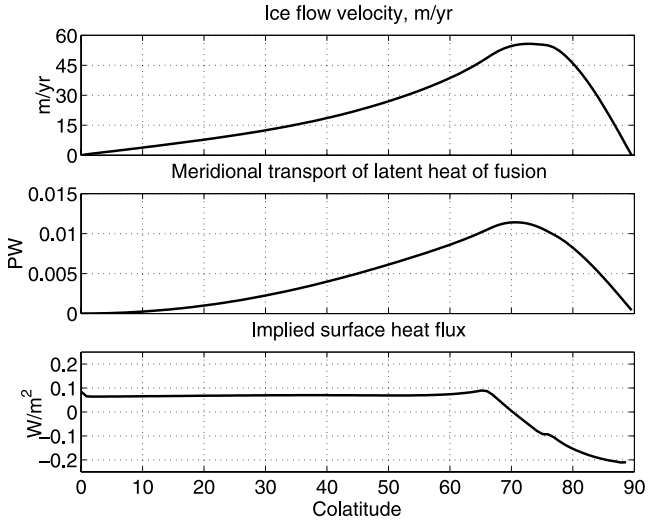

Figure 7. Same as Figure 3, but for the global ice-cover experiment.

warmed by geothermal input. In the absence of temperature gradients, lateral ocean heat transport must be zero.

[55] However, ocean heat transport could be important if open water exists. In this case, the ocean's surface boundary condition would not be isothermal, and thus temperature gradients and advective-diffusive heat fluxes can be sustained. This flux is not explicitly represented by our model, and would cause a thinning tendency near the ice margin. However, since poleward-flowing warm near-surface water would be rapidly cooled by contact with ice, it is not clear whether it would penetrate a large distance beyond the ice margin. Ice formed at high latitudes may remain thick and fast moving.

5.1.2. Ocean Circulation Feedbacks

[56] The freshwater released by the sea glacier at the tropics, and the brine rejected in the high-latitude freezing zone, may cause a significant ocean haline circulation. As we remarked above, this circulation is not likely to drive significant heat fluxes if ice cover is global, since no temperature gradients exist; however, an important ice-ocean feedback may occur in partly ice-covered situations.

5.1.3. Atmospheric Precipitation Feedback

[57] As ice cover advances and temperatures decline, evaporation shifts equatorward and declines in intensity, significantly modifying the global precipitation field. We parameterized this effect in a simple way in our model by shifting the precipitation field to follow the ice margin in the partly ice-covered experiment, and using a drastically reduced precipitation field in the totally glaciated experiment. This crude technique is a decent representation of the behavior of the FOAM GCM, but it ignores the possibility of a more complex interaction between ice cover and precipitation. On the other hand, snowfall is not the preeminent source of ice mass for a sea glacier: The bulk of the ice consists of frozen seawater. "Sea glaciers" would exist even if precipitation were zero.

[58] A proper resolution of these issues would require the coupling of the ice model to a full atmosphere-ocean GCM. This represents a considerable investment in model development effort, which would not be worthwhile if the sea glacier flow were miniscule. The present model demonstrates that ice-flow effects are likely to be worth considering: We are presently working to incorporate these effects into the FOAM GCM.

[59] The consequences of the ice flow described by our simple model are summarized below. We find that the flow of sea glaciers is a crucial factor in determining ice thickness in a Snowball Earth environment. Its heat and moisture fluxes may also be a significant driver of climate. We also speculate that flowing marine ice might also play a role in creating the distinctive geological features of Neoproterozoic glaciations.

5.2. Impact on Ice Thickness

[60] In a "partial snowball" environment, where tropical temperatures are above freezing, ice flows quickly from formation areas at high latitude to a melting zone at low latitude. This process limits ice thicknesses to a maximum of a few hundred meters. When ice cover is global, ice builds up to $\sim$1 km thickness; flow remains a crucial factor in determining ice distribution.

[61] The problem of ensuring the survival of photosynthetic organisms in a snowball climate persists. Flowing ice only makes the problem more acute, since small "refugia" of open water or thin ice would be invaded and perhaps overrun by flowing ice. Unless areas of open water existed that were too large to be invaded, we must find another refuge for photosynthetic life, perhaps within the ice itself or within geothermally warmed continental lakes.

[62] On the Ross ice shelf, crevasses form in regions of high strain resulting from the flow of ice around the Crary ice rise [*Barrett*, 1975]. Open water containing phytoplankton exists at the bottom of these crevasses. A similar process could occur on Snowball Earth, producing thin ice in crevassed zones near islands and continents. This may provide another biotic refugium, one which actually depends on flowing ice for its existence.

5.3. Implications for Climate and Ice Extent

[63] The rapid melting at the low-latitude terminus of the sea glacier in the partially glaciated experiment may be

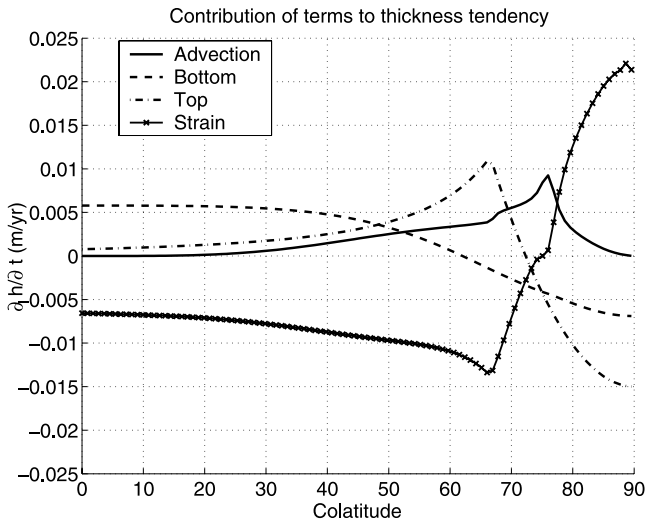

Figure 8. Same as Figure 4, but for the global ice-cover experiment.

climatically significant for two reasons. First, melting ice at the ice margin cools the atmosphere and ocean in that area. Second, the meltwater reduces sea-surface salinity, increasing stratification. This inhibits convection, reducing entrainment of warm water from below and causing a shallower mixed layer (with a smaller heat capacity). This leads to a larger sea-surface temperature drop in response to wintertime cooling. Both effects promote the expansion of sea ice into the melting zone.

[64] Coupled GCM simulations are required to find the response of the atmosphere-ice-ocean system to the ice sheet's heat and freshwater fluxes. However, we can roughly estimate the cooling caused by latent heat absorption. The local cooling must be balanced by reduced emission to space or by atmospheric heat transport. Radiative emission in the present-day atmosphere-ocean system is reduced by $\sim$2 W/m^2 per degree of surface temperature drop [*Barsugli and Battisti*, 1998]. Thus the latent heat transport is likely to cool the melting zone by several °C unless atmospheric heat transport is unusually efficient at resupplying heat to the melting zone. The 0°C isotherm is likely to move equatorward by several degrees latitude; the ice margin shifts in concert. Efficient atmospheric heat transport leads to a smaller temperature drop over a wider area.

[65] We may also gauge the magnitude of the freshwater flux released by the ice sheet. The peak meltwater supply rate (1.5 m/yr) is comparable to the annual-mean precipitation over the modern-day oceans [*Peixoto and Oort*, 1992]. The correlation of extreme sea ice coverage and the ''Great Salinity Anomalies'' in the North Atlantic during the 1970 and 1980s is well documented [*Belkin et al.*, 1998; *Deser and Blackmon*, 1993]. The freshwater delivered by our model's ice sheet can create a salinity anomaly as strong as the GSA in a circumglobal band 100 m deep and 100 km wide in a single year. With each successive year, this salinity anomaly grows stronger and wider. Coupled GCMs forced with meltwater fluxes one fourth as large as this have responded with an almost complete shutdown of the thermohaline circulation [*Manabe and Stouffer*, 2000]. (This observation demonstrates that the amount of meltwater in question strongly impacts ocean convection; we do not intend to draw conclusions about thermohaline circulation on Snowball Earth.)

[66] Even if melting and cooling caused only a small increase in ice extent, they would be amplified by the ice-albedo feedback. A small increase in ice extent leads to greater reflection of sunlight, reducing temperature and causing even more ice to form.

[67] Since existing GCMs do not consider the viscous flow of floating ice sheets, they lack these large heat and freshwater fluxes. Note that this effect is different from the issue of ''dynamic sea ice'' treated in some advanced GCMs, which deals with the wind- and current-driven motion of a thin layer of ice. The above estimates suggest that these fluxes may be large enough to significantly affect a GCM's equilibrium climate, increasing the likelihood of global ice cover. If realistic GCMs were able to attain global ice cover, it would not, of course, mean that the ''hard snowball'' state actually occurred.

5.4. Geological Implications

[68] A flowing sea glacier that becomes grounded on a continental shelf might lead to significant erosion as it slides over the seafloor. We speculate that some of the glacial erosion features reported by *Hoffman et al.* [1998] and other authors might result from erosion by sea glaciers.

[69] The Ghaub Formation is a Neoproterozoic glacial deposit that lies atop a large, thick platform of carbonate rock deposited in shallow water, similar to that found today in the Bahamas. The deposit is composed of carbonate debris from the underlying platform. The most substantial deposits lie on the slope adjacent to the platform.

[70] The most obvious cause of these glacial deposits is a continental glacier flowing out over a coastal carbonate platform. However, an ice sheet supplied by very weak net precipitation must have very slow ice flow speeds and thus weak erosion. With a simple equation balancing accumulation against outflow for a terrestrial ice sheet, we have found that for precipitation rates of 5 mm/year, an ice sheet 1 km thick at a radius of 2000 km from its center has a velocity of roughly 5 m/yr. This difficulty can be resolved by concluding that precipitation was indeed high, and that full Snowball conditions did not occur, or one may seek another erosive agent.

[71] *Hoffman and Schrag* [1999] propose an alternative explanation for the Ghaub deposits, involving purely local, vertical transport. They describe a sea ice layer freezing at its base and sublimating at the surface (as in *McKay*'s [2000] model); substrate material is frozen into the base of the ice layer, carried upward, and deposited at the ice surface as a sort of evaporite. This explanation is inadequate for the following reasons:

[72] 1. If the ice surface is covered with a rock layer, the layer's low albedo may spoil the ice-albedo feedback is crucial to maintaining Snowball Earth conditions. On the other hand, the limited area of these deposits may have little effect on global albedo.

[73] 2. Mud and loose stone can be incorporated into freezing ice and lifted. However, it is unclear whether this process can rip pieces from a structurally competent rock layer.

[74] 3. If rock is lifted and dropped in situ, why does the Ghaub carbonate platform have only thin, patchy glacial deposits on top, but thick layers of debris on the continental slopes around it?

[75] As an alternative to terrestrial ice sheets and to the ''sea-ice elevator'' described above, we ask whether flowing marine ice might be responsible for the glacial features seen in the Ghaub formation. We envision a global-scale sea glacier, moving toward the equator. Along the way, it encounters the carbonate platform. Erosion occurs as the ice sheet flows around or over parts of the platform. When the ice returns to deeper water and lifts off the bottom, glacial debris is be deposited on the slope, downstream (equatorward) from the platform.

[76] Flowing marine ice may be a much more effective erosive agent than a terrestrial ice sheet, since its flow velocity is an order of magnitude larger than that estimated for continental ice, and since the base of a marine ice layer is at the freezing point, rather than being frozen to the bed. If sea glaciers are responsible for glacial erosion, the absence of continental material in the glacial deposits would be an expected consequence of the marine origin of the ice. The thin, patchy debris layers on top of the platform may be explained by the continual removal of material by flowing

ice; till would accumulate along the downstream continental slope as the ice pushes debris off the edge of the platform and then floats away. Basal melting in the tropics would release debris frozen into the floating ice, forming dropstones.

[77] There are several potential problems with the marine ice erosion hypothesis. The rapid flow rate of a sea glacier is partly a consequence of the extra ice mass supplied at the pole by basal freezing, and partly a result of the lack of drag at the base of the ice sheet. Would flow velocities remain high once the sea glacier becomes grounded? The onset of Neoproterozoic glaciation is accompanied by a sea-level drop. If this drop was large enough, the carbonate platform would have been well above sea level, out of reach of floating marine ice. However, sea glaciers could continue to erode the edges of the platform.

[78] One way to distinguish between erosion by marine and continental ice is to identify the ice flow direction. Our model predicts ice flow from pole to equator, whereas a continental glacier flows outward from the continent. In some cases, flow direction should be estimable from the orientation of glacial scouring features and the location of till deposition on the slope. Some paleogeographic reconstructions do indicate seaward ice flow [*Hambrey and Harland*, 1981; *Lemon and Gostin*, 1990; *Christie-Blick*, 1983], while in others [*Coats*, 1981], flow from deeper toward shallower water is inferred. Note, though, that these reconstructions are not always well constrained, and seaward ice flow is sometimes assumed a priori (P. Hoffman, personal communication, 2003.)

[79] In other cases, one may deduce flow direction by comparing the composition of glacially transported clasts in the till to that of nearby substrate material. Variations in the carbonate substrate and subglacial outcrops of non-carbonate materials may be mapped, and compared with maps of till composition to infer till transport direction [*Clark*, 1987].

[80] While detailed mapping is needed to draw a robust conclusion, P. F. Hoffman (personal communication, 2003) has noted that the Ghaub clasts are predominantly composed of oolite and robust stromatolite, materials formed along windward platform margins. This suggests strong erosion along the margin of the platform, consistent with sea glacier action. On the other hand, a very small fraction of granitic clasts is present [*Condon et al.*, 2002], which probably indicates a contribution from continental ice sheets, though a small outcrop of basement rock exists near the shelf edge [*Hoffman et al.*, 1998; P. F. Hoffman, personal communication, 2003] and provides a potential non-continental source.

[81] At present, we have no incontrovertible evidence that sea glaciers are either wholly or partly responsible for observed Neoproterozoic glacial features. However, our model leads us to expect thick, flowing sea ice in both the partly- and the totally-frozen cases. The possibility is thus worth considering when examining geological data.

6. Conclusion

[82] Thick layers of floating ice tend to deform under their own weight. The flow of these ''sea glaciers'' may strongly influence Snowball Earth climate. In particular, it may help to explain the discrepancy between GCM simulations, which fall short of global glaciation, and the observations and mechanisms that suggest or require total ice cover. Marine ice flow may also be responsible for glacial erosion of shallow carbonate platforms in a Snowball Earth regime. This hypothesis resolves some outstanding discrepancies between observations and existing mechanisms; however, it has not yet been adequately tested against the rock record. While our erosion hypothesis is highly speculative, we are more confident that marine ice flow is a major player in Snowball Earth transition climates, and that it significantly affects the equilibrium ice thickness during a Snowball Earth episode.

Appendix A: Temperature-Dependence of Rheology Constant

[83] The viscosity parameter in equation (3) depends on temperature in the following way [*Weertman*, 1957]:

$$\mu = \frac{\rho_i g(1-\rho_i/\rho_w)}{4\overline{A}},$$

where ρ_i and ρ_w are the densities of ice and water, and $\overline{A}$ is the depth-averaged value of the Glen flow law parameter A.

$$\overline{A} = \frac{1}{h}\int_{-h}^{0} A(T(z))dz. \tag{A1}$$

A is a function of temperature (T in Kelvin),

$$A = A_0 e^{-Q/RT}.$$

We use values for the constants A_0 and Q taken from *Barnes et al.* [1971]: $A_0 = 3.61 \times 10^{-13}$ Pa^{-3}/s, $Q = 60 \times 10^3$ J/mol when $T < 263.15$; $A_0 = 1.734 \times 10^3$ Pa^{-3}/s, $Q = 139 \times 10^3$ J/mol when $T \geq 263.15$.

[84] As it stands, this equation depends on the prognostic variable h, and so must be recomputed at each time step. However, we may eliminate this dependence as follows. The interior temperature profile is given by equation (4); note that since $h \gg z_0$, we may write T as a sum of a thin exponential solar boundary layer plus a linearly sloped interior solution.

$$T \approx T_s' + (T_f - T_s')\frac{z}{h} + \Delta_s e^{-z/z0}$$

$$T_s' = T_s - \Delta_s.$$

T_f is the temperature at the base of the ice, T_s' is the temperature just below the solar boundary layer, and Δ_s is the temperature jump across the boundary layer. Plugging the above expression for T into equation (4), to balance the two exponential terms in the equation we must have

$$\Delta_s = z_0 S_0(1-a)(1-r)/\kappa. \tag{A2}$$

We may now replace the depth-integral in equation (A1) with a temperature integral,

$$\overline{A} = \frac{1}{h}\int_{-h}^{0} A(T(z))dz = \frac{1}{h}\int_{T_f}^{T_s} A(T)\frac{\partial z}{\partial T}dT.$$

[85] The thinness of the solar boundary layer and the large heat input there means that within the boundary layer ($T_s' > T > T_s$), $\partial z/\partial T$ is nearly zero compared to its value in the interior. Thus we may modify the limits of the integral,

$$\overline{A} \approx \frac{1}{h}\int_{T_f}^{T_s'} A(T)\frac{\partial z}{\partial T}dT.$$

Since $\frac{\partial z}{\partial T} \approx$ constant $= h/(T_f - T_s')$ in the interior,

$$\overline{A} \approx \frac{1}{T_f - T_s'}\int_{T_f}^{T_s'} A(T)dT.$$

This approximation does not depend on h or z: $\overline{A}$ is a function of the external parameters T_f and T_s' alone. Thus we do not need a two-dimensional grid to resolve the vertical temperature profile, and we can pre-compute $\mu(\theta)$ once at the start of the model run, and use it throughout the integration.

Appendix B: Derivation of Flow Equation for Global Ice Cover

[86] As discussed in section 4, the ice flow law (equation (7)) is invalid when ice cover is global. When the ice sheets in each hemisphere meet at the pole, they exert a restraining force on each other, which brings ice velocity to zero at the equator. This restraining force is not included in the derivation of equation (7); we must re-derive it with this extra term.

[87] Our derivation is an extension of [*Weertman*, 1957], which finds the horizontal strain rate K for an ice shelf confined within a channel with parallel frictionless walls. We do not repeat the derivation of that work here. We follow Weertman's procedure for finding K in terms of the horizontal normal stress in the downstream direction σ_{xx}, obtaining

$$\sigma_{xx} = 2AK^{1/n} - \rho_i g(h - y), \tag{B1}$$

where A is the constant in Glen's flow law, ρ_i is ice density, and y is the height above the base of the ice shelf.

[88] Here σ_{xx} is found by balancing the stress within the ice sheet with the forces applied at the downstream ice edge. In Weertman's [1957] case, the integral of the stress σ_{xx} is balanced by integrated hydrostatic pressure in the water in which the ice is floating,

$$\int_0^h \sigma_{xx}dy = -\int_0^{h\rho_i/\rho_w} \rho_w g(h\rho_i/\rho_w - y)dy,$$

where ρ_w is the density of water. However, in our case, we have an additional force: a back-pressure supplied by the counteracting ice sheet in the opposite hemisphere. Thus the force balance above becomes

$$\int_0^h \sigma_{xx}dy = -\int_0^{h\rho_i/\rho_w} \rho_w g(h\rho_i/\rho_w - y)dy + F_b, \tag{B2}$$

where F_b is the back-pressure force per unit distance along the equator. Inserting equation (B1) into equation (B2) gives

$$2\overline{A}K^{1/n}h - g\rho_i h^2/2 = -\rho_w g\frac{(h\rho_i/\rho_w)^2}{2} + F_b,$$

where $\overline{A} = h^{-1}\int_0^h A$. Solving for K,

$$K = \left[\frac{gh\rho_i}{4\overline{A}}(1 - \rho_i/\rho_w) + \frac{F_b}{2\overline{A}h}\right]^n.$$

Defining

$$\mu \equiv \frac{g\rho_i(1 - \rho_i/\rho_w)}{4\overline{A}}; \qquad b \equiv \frac{2F_b}{g\rho_i(1 - \rho_i/\rho_w)}$$

gives

$$K = \mu^n(h - b/h)^n.$$

When $b = 0$, we recover Weertman's result. This expression is used to compute the flow divergence in section 4.

[89] **Acknowledgments.** We wish to thank D. R. MacAyeal for advice on ice-shelf modeling, and for suggesting ice-shelf crevasses as a biotic refugium; S. G. Warren for the term "sea glacier" and insight regarding solar penetration in ice; B. Hallet for information on glacial erosion; P. Hoffman and A. M. Ziegler for information on Neoproterozoic carbonate geology; and N. Christie-Blick and an anonymous reviewer for their extremely helpful comments on the manuscript.

References

Barnes, P., D. Tabor, and J. C. F. Walker, Friction and creep of polycrystalline ice, *Proc. R. Soc. London*, *324*(1557), 127–155, 1971.

Barrett, P. J., Seawater near the head of the Ross Ice Shelf, *Nature*, *256*, 390–392, 1975.

Barsugli, J. J., and D. S. Battisti, The basic effects of atmosphere-ocean thermal coupling on midlatitude variability, *J. Atmos. Sci.*, *55*(4), 477–493, 1998.

Belkin, I. M., S. Levitus, J. Antonov, and S.-A. Malmberg, "Great Salinity Anomalies" in the North Atlantic, *Prog. Oceanogr.*, *41*, 1–68, 1998.

Chandler, M. A., and L. E. Sohl, Climate forcings and the initiation of low-latitude ice sheets during the Neoproterozoic Varanger glacial interval, *J. Geophys. Res.*, *105*(D16), 20,737–20,756, 2000.

Christie-Blick, N., Glacial-marine and subglacial sedimentation, Upper Proterozoic Mineral Fork Formation, Utah, in *Glacial-Marine Sedimentation*, edited by B. F. Molinia, pp. 703–776, Plenum, New York, 1983.

Christie-Blick, N., L. E. Sohl, and M. J. Kennedy, Considering a Neoproterozoic Snowball Earth, *Science*, *298*, 1087, 1999.

Clark, P. U., Subglacial sediment dispersal and till composition, *J. Geol.*, *95*(4), 527–541, 1987.

Coats, R. P., Late Proterozoic (Adelaidean) tillites of the Adelaide Geosyncline, in *Earth's Pre-Pleistocene Glacial Record*, edited by M. J. Hambrey and W. B. Harland, Cambridge Univ. Press, New York, 1981.

Condon, D. J., A. R. Prave, and D. I. Benn, Neoproterozoic glacial-rainout intervals: Observations and implications, *Geology*, *30*, 35–38, 2002.

Crowley, T. J., and S. K. Baum, Effect of decreased solar luminosity on late Precambrian ice extent, *J. Geophys. Res.*, *98*(D9), 16,723–16,732, 1993.

Crowley, T. J., and W. T. Hyde, CO_2 levels required for deglaciation of a "Near-Snowball" Earth, *Geophys. Res. Lett.*, *28*, 283–286, 2001.

Deser, C., and M. Blackmon, Surface climate variations over the North Atlantic Ocean during winter: 1900–1989, *J. Clim.*, *6*, 1743–1753, 1993.

Evans, D. A. D., Stratigraphic, geochronological, and paleomagnetic constraints upon the Neoproterozoic climatic paradox, *Am. J. Sci.*, *300*(5), 347–433, 2000.

Gaidos, E. J., K. H. Nealson, and J. L. Kirschvink, Life in ice-covered oceans, *Science*, *284*, 1631–1633, 1999.

Halverson, G. P., P. F. Hoffman, D. P. Schrag, and A. J. Kaufman, A major perturbation of the carbon cycle before the Ghaub glaciation (Neoproter-

ozoic) in Namibia: Prelude to Snowball Earth?, *Geochem. Geophys. Geosyst.*, 3, Paper number 2001GC000244, 2002. (Available at http://gcubed.magnet.fsu.edu/main.html)

Hambrey, M. J., and W. B. Harland, *Earth's Pre-Pleistocene Glacial Record*, Cambridge Univ. Press, New York, 1981.

Hoffman, P. F., and D. P. Schrag, Considering a Neoproterozoic Snowball Earth: Reply, *Science*, *284*, 1087–1088, 1999.

Hoffman, P. F., and D. P. Schrag, The Snowball Earth hypothesis: Testing the limits of global change, *Terra Nova*, *14*, 129–155, 2002a.

Hoffman, P. F., A. J. Kaufman, G. P. Halverson, and D. P. Schrag, A neoproterozoic Snowball Earth, *Science*, *281*, 1342–1346, 1998.

Hoffman, P. F., G. P. Halverson, and J. P. Grotzinger, Are Proterozoic cap carbonates and isotopic excursions a record of gas hydrate destabilization following Earth's coldest intervals?: Comment, *Geology*, *30*, 761–762, 2002b.

Hyde, W. T., T. J. Crowley, S. K. Baum, and W. R. Peltier, Neoproterozoic 'Snowball Earth' simulations with a coupled climate/ice-sheet model, *Nature*, *405*, 425–429, 2000.

Jacob, R., C. Schafer, I. Foster, M. Tobis, and J. Anderson, Computational design and performance of the Fast Ocean Atmosphere Model, version 1, in *Proceedings of the 2001 International Conference on Computational Science*, edited by V. N. Alexandrov, J. J. Dongarra, and C. J. K. Tan, pp. 175–184, Springer-Verlag, New York, 2001.

Kennedy, M. J., N. Christie-Blick, and A. R. Prave, Carbon isotopic composition of Neoproterozoic glacial carbonates as a test of paleoceanographic models for snowball Earth phenomena, *Geology*, *29*, 1135–1138, 2001a.

Kennedy, M. J., N. Christie-Blick, and L. E. Sohl, Are Proterozoic cap carbonates and isotopic excursions a record of gas hydrate destabilization following Earth's coldest intervals?, *Geology*, *29*, 443–446, 2001b.

Kennedy, M. J., N. Christie-Blick, and L. E. Sohl, Are Proterozoic cap carbonates and isotopic excursions a record of gas hydrate destabilization following Earth's coldest intervals?: Reply, *Geology*, *30*, 763, 2002.

Kirschvink, J. L., Late Proterozoic low-latitude global glaciation: The Snowball Earth, in *The Proterozoic Biosphere*, edited by J. W. Schopf and C. Klein, pp. 51–52, Cambridge Univ. Press, New York, 1992.

Knoll, A. H., J. M. Hayes, A. J. Kaufman, K. Swett, and I. B. Lambert, Secular variation in carbon isotope ratios from upper Proterozoic successions of Svalbard and East Greenland, *Nature*, *321*, 832–838, 1986.

Lemon, N. M., and V. A. Gostin, Glacigenic sediments of the late Proterozoic Elatina Formation and equivalents, Adelaide Geosyncline, South Australia, in *The Evolution of a Late Precambrian-Early Paleozoic Rift Complex: The Adelaide Geosyncline*, pp. 149–163, Geol. Soc. of Australia, Sydney, N.S.W., Australia, 1990.

Lubick, N., Snowball fights, *Nature*, *417*, 12–13, 2002.

Macayeal, D., and V. Barcilon, Ice shelf response to ice stream discharge fluctuations: I. Unconfined ice tongues, *J. Glaciol.*, *34*(116), 121–127, 1988.

Manabe, S., and R. J. Stouffer, Study of abrupt climate change by a coupled ocean-atmosphere model, *Quat. Sci. Rev.*, *19*, 285–299, 2000.

McKay, C. P., Thickness of tropical ice and photosynthesis on a Snowball Earth, *Geophys. Res. Lett.*, *27*, 2153–2156, 2000.

McKay, C. P., G. D. Clow, and S. W. Squyres, Thickness of ice on perennially frozen lakes, *Nature*, *313*, 561–562, 1985.

Peixoto, J. P., and A. H. Oort, *Physics of Climate*, Am. Inst. of Phys., College Park, Md., 1992.

Peltier, W. R., A Neoproterozoic Snowball Earth: Impacts of a dynamic ocean, *EOS Trans. AGU*, *82*(20), Spring Meet Suppl., S8, 2001.

Peltier, W. R., *Encyclopedia of Global Environmental Change*, vol. 1, *Earth System History*, edited by M. C. McCracken and J. S. Perry, pp. 31–60, John Wiley, Hoboken, N.J., 2002.

Poulsen, C. J., R. T. Pierrehumbert, and R. L. Jacob, Impact of ocean dynamics on the simulation of the Neoproterozoic "Snowball Earth," Geophys, *Res. Lett.*, *28*, 1575–1578, 2001.

Schmidt, P. W., and G. E. Williams, The Neoproterozoic climatic paradox: Equatorial paleolatitude for Marinoan glaciation near sea level in South Australia, *Earth Planet. Sci. Lett.*, *134*, 107–124, 1995.

Schrag, D., and P. F. Hoffman, Life, geology, and Snowball Earth, *Nature*, *409*, 306, 2001.

Sohl, L. E., and N. Chistie-Blick, Paleomagnetic polarity reversals in Marinoan (ca. 600 Ma) glacial deposits of Australia: Implications for the duration of low-latitude glaciation in Neoproterozoic time, *GSA Bull.*, *111*(8), 1120–1139, 1999.

Thomas, R. H., and D. R. MacAyeal, Derived characteristics of the Ross Ice Shelf, Antarctica, *J. Glaciol.*, *28*(100), 397–412, 1982.

Trenberth, K. E., and J. M. Caron, Estimates of meridional atmosphere and ocean heat transports, *J. Clim.*, *14*, 3433–3443, 2001.

van de Wal, R. S. W., Mass-balance modelling of the Greenland ice sheet: A comparison of an energy-balance model and a degree-day model, *Ann. Glaciol.*, *23*, 36–45, 1996.

Weertman, J., Deformation of floating ice shelves, *J. Glaciol.*, *3*(21), 38–42, 1957.

Young, G. M., Iron-formation and glaciogenic rocks of Rapitan Group, Northwest Territories, Canada, *Precambrian Res.*, *3*(2), 137–158, 1976.

J. C. Goodman and R. T. Pierrehumbert, 5731 South Ellis Avenue, University of Chicago, Chicago, IL 60637, USA. (goodmanj@uchicago.edu; rtp1@geosci.uchicago.edu)